AAPS PharmSciTech, Vol. 13, No. 2, June 2012 (© 2012)
DOI: 10.1208/s12249-012-9788-1

Research Article

Development of Mannosylated Liposomes Using Synthesized *N*-Octadecyl-D-Mannopyranosylamine to Enhance Gastrointestinal Permeability for Protein Delivery

Wasu Witoonsaridsilp,[1] Ornlaksana Paeratakul,[2] Busaba Panyarachun,[3] and Narong Sarisuta[1,4]

Received 11 January 2012; accepted 4 April 2012; published online 5 May 2012

Abstract. The lysozyme (LZ)-entrapped mannosylated liposomes were prepared in this study by the use of *N*-octadecyl-D-mannopyranosylamine (SAMAN), which had been synthesized in-house and confirmed by characterization with FTIR and NMR. The reactant residues of synthesized SAMAN were found to be less than 1%. The mean sizes, zeta potentials, drug entrapment efficiencies, and loading capacities of all liposomal formulations were in the ranges of 234.7 to 431.0 nm, −10.97 to −25.80 mV, 7.52 to 14.10%, and 1.44 to 2.77%, respectively. The permeability of mannosylated LZ liposomes across Caco-2 cell monolayers was significantly enhanced to about 2.5- and 7-folds over those of conventional liposomes and solution, respectively, which might be due to the role of mannose receptor or mannose-binding protein on the intestinal enterocytes.

KEY WORDS: Caco-2 cells; lysozyme; mannosylated liposomes; *N*-octadecyl-D-mannopyranosylamine; permeation.

INTRODUCTION

Oral peptide and protein drug delivery still remain the area of challenges for pharmaceutical scientists due to their low stability and permeability in gastrointestinal (GI) tract. One among promising strategies to improve GI permeability by employing colloidal microcarriers is the utilization of liposomes for oral delivery of peptide and protein drugs (1–5). Specific receptor-mediated drug targeting would be another approach to improve oral drug absorption by modifying particulate system such as liposomes with specific ligand. There were many attempts to deliver non-specific and specific drug targeting to specialized M cells. However, major disadvantages of this strategy reside in that majority of intestinal M cells are located at the base of villous and as such located in a restricted site of intestinal wall so that M cells areas are presented in only low numbers (less than 1% of all enterocytes) (6).

It has been reported that particulate drug carriers could not only be taken up by Peyer's patches, but also *via* the normal intestinal enterocytes area (7). It was suggested that some molecules, *i.e.*, wheat germ agglutinin, Con A, and binding subunit of *E. coli* heat-labile toxin-conjugated nanoparticles could bind and transport across intestinal epithelial cells such as Caco-2 cells (6). As specific targeting, glycotargeting concepts are basically either relied on the oligosaccharide moiety or lectin as a component of drug delivery system (1). In this regard, modified liposomes with sugar moiety as mannosylated ligand might be able to target to the absorption site and enhance the intestinal absorption of protein drugs. The possible rationale is the pattern recognition receptor, mannose receptors (MR), or mannose-binding proteins (MBP), which would be predominantly presented on macrophages, hepatic tissues, and serum capable of recognizing and internalizing mannose, fucose, and *N*-acethylglucosamine terminated molecules (8). The expression of MR or MBP could also be found on numerous tissues including intestinal epithelium (9). The emerging of MR or MBP on intestinal epithelial cells was substantially evidenced, *i.e.*, especially abundant on villous epithelial cells of mouse intestine in duodenum and ileum (10).

The purpose of this investigation was to develop mannosylated liposomes, which are able to exhibit a strong bioadhesive property to MR expressed on gut mucosal tissue, in order to improve gastrointestinal permeability of the model protein lysozyme. The mannosylating ligand, *N*-octadecyl-D-mannopyranosylamine, was synthesized in-house. The physicochemical characterizations and permeation studies across Caco-2 cell monolayers of mannosylated lysozyme liposomes compared to free drug were subsequently carried out.

MATERIALS

Lysozyme (LZ) from chicken egg white (L7651) was purchased from Sigma-Aldrich Chemie, Steinheim, Germany.

[1] Department of Manufacturing Pharmacy, Faculty of Pharmacy, Mahidol University, 447 Sri-Ayudhya Road, Bangkok, 10400, Thailand.
[2] Department of Pharmaceutical Technology, Faculty of Pharmacy, Srinakharinwirot University, 63 Rangsit-Nakhonnayok Road, Nakhonnayok, 26120, Thailand.
[3] Department of Anatomy, Faculty of Medicine, Srinakharinvirot University, 23 Sukhumvit Road, Bangkok, 10110, Thailand.
[4] To whom correspondence should be addressed. (e-mail: pynst@mahidol.ac.th)

Phosphatidylcholine (PC) (Phospholipon® 90G) was kindly provided by Rhone-Poulenc Rorer, Köln, Germany. Cholesterol (Chol), sodium dihydrogen phosphate, and disodium hydrogen phosphate were supplied by Merck, Darmstadt, Germany. Dicetyl phosphate (DCP), stearylamine, and D-mannose were obtained from Fluka, Steinheim, Germany. Caco-2 cell line (HTB-37) was purchased from ATCC, Manassas, VA, USA. Dulbecco's modified Eagles medium (D-MEM) was supplied by Gibco®, USA. Fetal bovine serum was purchased from HyClone®, Thermo scientific, Cramlington, UK. Antibiotic solutions (10,000 U/ml penicillin G, streptomycin 10 mg/ml) and trypsin–EDTA were obtained from PAA, Austria. *N*-hydroxyethylpiperazine-*N*′-2-ethane sulfonate (HEPES) was purchased from Research Organics, USA. All chemicals used were of analytical or reagent grade.

METHODS

Synthesis and Characterization of *N*-Octadecyl-*d*-Mannopyranosylamine

The synthesis procedure was carried out with slight modification according to the previous report (11). A 5 mmol amount of stearylamine was dissolved in 15 ml ethanol and heated up to 70 °C, after which 5 mmol of D-mannose was added with continuous stirring. This solution was continuously stirred further for 15 min after sugar had completely dissolved. Subsequently, this solution was cooled down to 40 °C and diluted with 35 ml hexane. The obtained crystals were collected at room temperature and washed with 30 ml hexane before drying under diminished pressure.

The Fourier transform infrared spectroscopy (FTIR) spectra of mannose, stearylamine, and *N*-octadecyl-D-mannopyranosylamine (SAMAN) were determined by the use of FTIR spectrophotometer (Nicolet® 6700 FTIR Spectrometer, WI, USA). The ^{1}H nuclear magnetic resonance (NMR) spectroscopy (Bruker® AV-300, Rheinstätten, Germany) was performed at room temperature in Fourier transform mode using deuterated pyridine as a solvent at 500 MHz.

The residual mannose in synthesized SAMAN was determined by using high-performance liquid chromatography (HPLC) pre-column derivatization technique as previously described (12). The derivatized sample solution was diluted with dimethylformamide before injected into the chromatographic reversed phase(C_{18}) column (Mightysil® ODS RP-C18, 5 μm, 4.6×250 mm, Kanto Chemical, Tokyo, Japan) on an HPLC system equipped with a high-precision pump (LC-20AD, Shimadzu, Kyoto, Japan), UV–vis detector (SD20A, Shimadzu), and system controller (LC-20AD, Shimadzu). The 70:30 (*v*/*v*)—acetonitrile/water was used as a mobile phase at a flow rate of 1.0 ml/min with the detection wavelength at 240 nm. In addition, the residual sterylamine could also be analyzed by HPLC as previously described (13). The derivatized sample solution was diluted with acetonitrile before injected into the chromatographic reversed phase (C_{18}) column. The 98:2 (*v*/*v*)—acetonitrile/water was used as a mobile phase at a flow rate of 1.4 ml/min with the detection wavelength at 240 nm.

Preparation of Mannosylated LZ Liposomes

Mannosylated LZ liposomes containing SAMAN at 5% (mannosylated-0.5), 7.5% (mannosylated-0.75), and 10% (mannosylated-1) were prepared by using thin film method. Total lipid mixtures of 20 mmol containing PC, Chol, DCP, and SAMAN at molar ratios of 8:2:1:0.5, 8:2:1:0.75, and 8:2:1:1 were dissolved in 2:1 (*v*/*v*)—chloroform/methanol in a ground-glass quick-fit neck boiling flask. The solvent was evaporated at 30–35 °C under reduced pressure by using a rotary evaporator (Eyela® N-1000 Series, Tokyo Rikakikai, Japan). After the thin film was obtained, drying was continued for at least 1 h in the evaporator to completely remove the remaining trace of organic solvent. The lipid film was then rehydrated with 10 ml of 3 mg/ml LZ in phosphate buffer pH 7.4 at 25–30 °C for 30 min. The liposomal dispersions were subsequently extruded six times through 100-nm pore size polycarbonate membranes (Cyclopore®128, Whatman, NJ, USA) by using a membrane extruder (Lipex®, Northern Lipids, Vancouver, BC, Canada).

Physicochemical Characterization of Mannosylated LZ Liposomes

The microscopic appearance of the vesicles was examined using negative stain transmission electron microscope (TEM; Jeol® JEM-2100, Jeol, Tokyo, Japan). Particle size of LZ liposomes were determined at 25±0.1 °C with a particle analyzer (Zetasizer® NanoSeries, Malvern Instrument, Malvern, UK) equipped with a 4 mW He/Ne laser (λ=633 nm). The intensity of the laser light scattered by the samples was detected at an angle of 173° by a photomultiplier. The zeta potentials were assessed by determining the electrophoretic mobility of particles and calculated by using the Helmholtz–Smoluchowsky equation (Zetasizer®NanoSeries, Malvern Instrument). All determinations were performed in triplicate.

The entrapment efficiency (%EE) and loading capacity (%LC) of LZ liposomes were determined by using ultracentrifugation (Optimal L-80 XP Preparative Ultracentrifuge, Beckman, UK) at 50,000 rpm for 40 min. The pellets were then resuspended in buffer and repeatedly centrifuged until LZ concentration in the filtrate was lower than 3.0% of total amount added into the formulation. Triton X-100 was used to liberate LZ from liposomes and the protein contents in solution were then analyzed by using Lowry-Peterson assay at 750 nm (14).

Permeation Studies Across Caco-2 Cell Monolayers

Caco-2 cells were grown in 75-cm^2 culture flask (Corning Costar®, NY, USA) at 37 °C in an atmosphere of 5% CO_2 using Dulbecco's modified eagle medium (D-MEM) at pH 7.2. The medium was supplemented with 4.5 g/l D-glucose, 584 mg/ml L-glutamine, 1% penicillin–streptomycin, HEPES 25 mM, and 10% fetal bovine serum. The medium was changed every other day until the flask reached 90% confluence. The cells were washed with phosphate buffer saline (PBS) and removed from the flasks by incubating with 0.5% trypsin in 0.2% EDTA solution for 4–5 min at 37 °C. The cells were collected into the centrifugation tubes, spun for 10 min at 1,250 g, and the pellets were then resuspended in D-MEM.

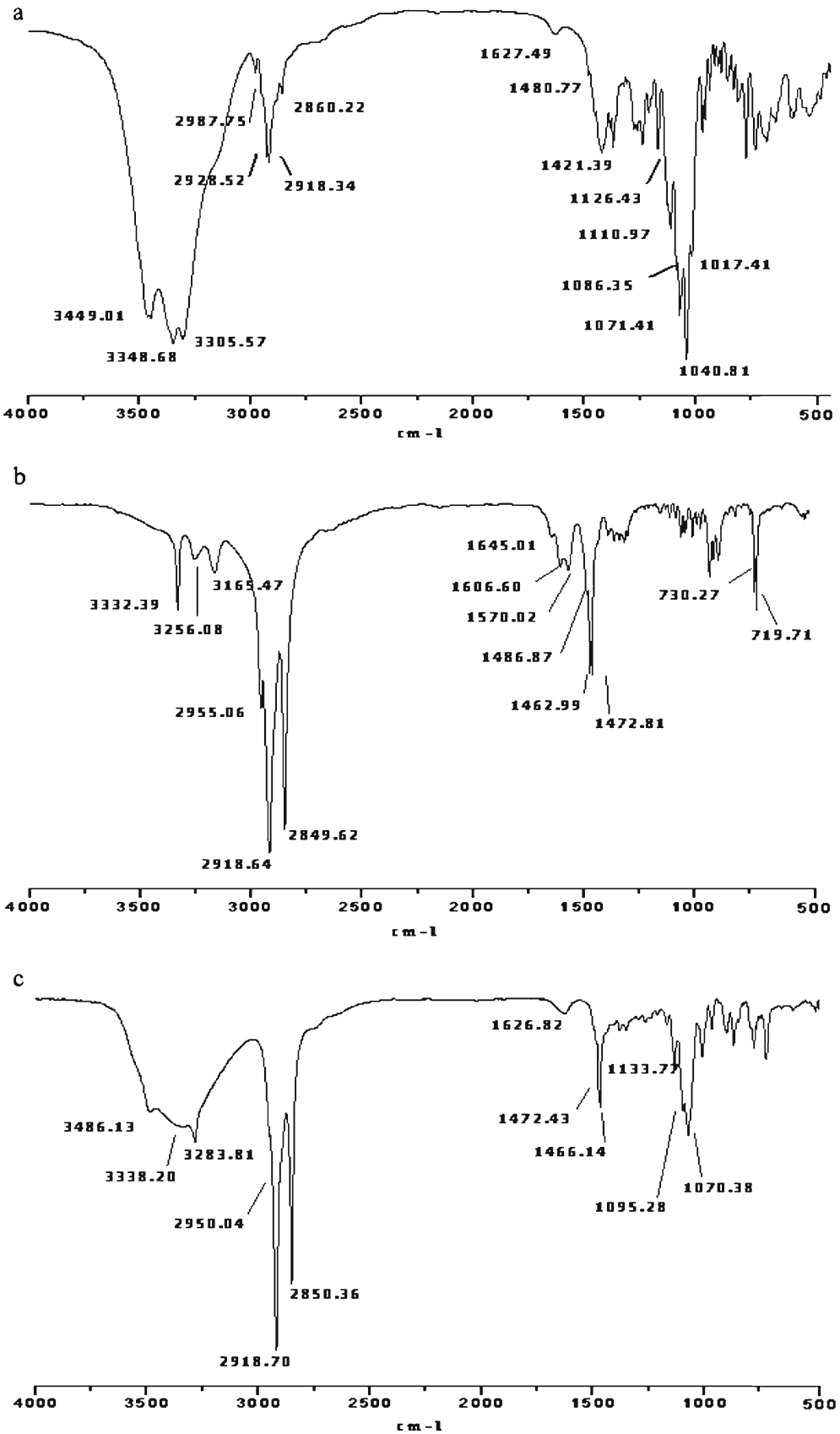

Fig. 1. FTIR spectra of **a** mannose, **b** stearylamine, and **c** SAMAN

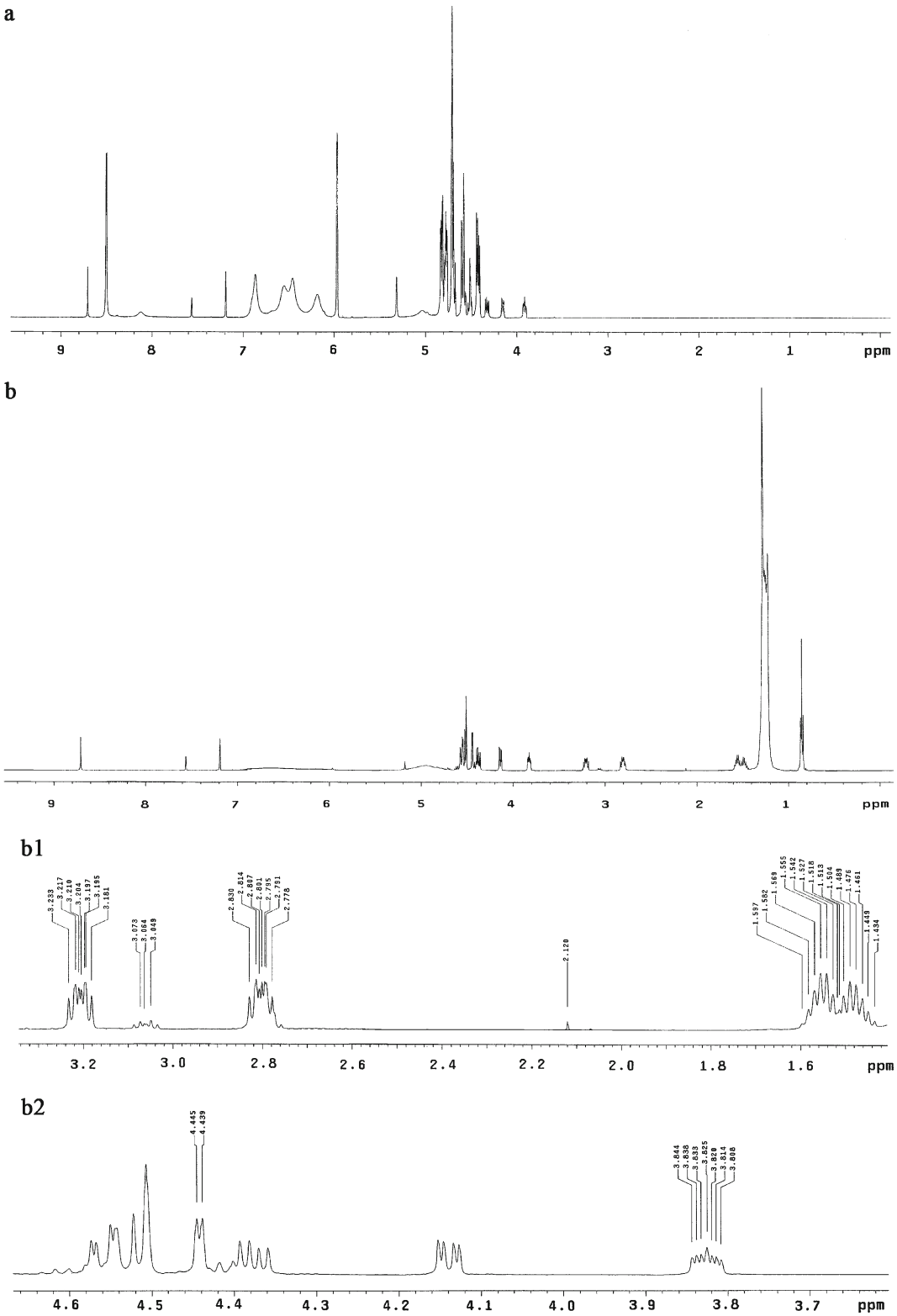

Fig. 2. The chemical shifts of ^{1}H NMR spectra of **a** mannose and **b** SAMAN; (*b1*) indicated small intensity at δ 2.12 ppm, and (*b2*) indicated multiplex at δ 3.83 ppm and duplet at δ 4.45 ppm, determined in d_5-pyridine solvent

The Caco-2 cells at 20–40 passages were seeded on the permeable polycarbonate insert of 1-cm^2 membrane size and 0.4-μm pore size placed in 12-mm Transwell® plate (Corning Costar®) at 100,000 cells/cm^2. The inserts were fed with complete media every other day and then were used in the experiments 18–28 days after seeding. The integrity of the cell monolayers was evaluated by measuring transepithelial electrical resistance (TEER) value with a volt/ohm meter

(Millicell®-ERS, Millipore, MA, USA). The cell inserts were used experimentally when the resistance reached 300–600 Ω cm^2 (3). The TEER values were measured again after transport experiments to verify the integrity of the cell monolayers. The last medium replacement had been accomplished 24 h before the transport studies started. Before the experiments, the cell monolayers were washed with PBS and transport medium (Hank's balance salt solution, HBSS, containing 25 mM HEPES and 25 mM glucose). The pH's of apical and basolateral media were 6.8 and 7.4, respectively. After each wash, the plates were incubated with the transport medium for 15 min at 37 °C, and then TEER value was measured. After TEER measurements, the incubation media in both sides of the cell monolayer were removed by aspiration. An aliquot of LZ solution or liposomal preparations in HBSS pH 6.8 was added to the apical side and transport medium without drug to the basolateral side. Aliquot portions of medium in basolateral side were collected at various time intervals and analyzed by HPLC. These aliquots were spiked with LZ standard solution in HBSS pH 7.4 before injected into HPLC. All samples were analyzed within 24 h after transport studies.

The contents of LZ from transport studies were analyzed as previously described (15) by an HPLC system equipped with a high-precision pump (LC-20AD, Shimadzu), UV–vis detector (SD20A, Shimadzu), and system controller (LC-20AD, Shimadzu). A C_5 reverse-phase column (Jupitor®, 5 μm, 300 Å, 4.6×250 mm, Phenomenex, CA, USA) was used at ambient temperature. The mobile phase was 0.1% trifluoroacetic acid in acetonitrile: 0.1% trifluoroacetic acid in water, which was eluted at a flow rate of 1.0 ml/min with a gradient of 25:75 to 50:50 (*v*/*v*) from 0 to 15 min, 50:50 to 100:0 from 15 to 25 min, and eluted back to the starting ratio from 25 to 35 min. Column was further equilibrated for another 10 min. The sample injection volume was 50 μl and the detection wavelength was 220 nm. The retention time was about 14 min and the runtime was 45 min.

RESULTS AND DISCUSSION

Synthesis and Characterization of *N*-Octadecyl-*d*-Mannopyranosylamine

The reaction from unprotected sugars of mono- or oligosaccharide with long chain fatty amine in hot alcoholic solution has been described (11). In this procedure, the reaction was achieved at unprotected anomeric hydroxyl group of mannose with stearylamine, resulting in occurrence of amine bond of secondary glycosylamine. The synthesized SAMAN obtained was pale yellow crystals with the yield from 73.97–76.48% by weight based on the net weight of the initial reactants.

It can be seen in Fig. 1 that the FTIR spectrum of mannose had the broad intense band around 3,500–3,300 cm^{-1} and sharp peaks between 3,000 and 2,800 cm^{-1}. These signals indicated the hydroxyl stretching vibration and $–CH_3$ and $–CH_2–$ stretching, respectively. In addition, the signal at lower wave number at 1,150–1,085, 1,124–1,087, and 1,085–1,050 cm^{-1} exhibited the characteristics of C–O stretching of either, primary and secondary alcohol, and secondary alicyclic five- or six-membered ring, respectively. The FTIR spectrum of stearylamine possessed the characteristics of NH stretching vibration as evidenced by the sharp peak between 3,500 and 3,200 cm^{-1}. Accordingly, the band position between 3,000 and 2,800 cm^{-1}represented the $–CH_3$ and $–CH_2–$, which was more intense compared to that of mannose due to the long alkyl chain. Other important peaks were NH bending around 1,650–1,580 cm^{-1}. These bands were pronounced in primary amine. Peak around 1,486–1,462 cm^{-1} could be identified as CH_2 bending characteristics. Considering the spectrum of synthesized SAMAN, the intense broadband around 3,500–3,000 cm^{-1} was decreased with respect to that of mannose along with the emerging of one single broad band. These might be due to the combination of OH stretching of mannose molecules and NH stretching of the amine. The area of NH bending between 1,650 and 1,580 cm^{-1} was also diminished compared to that of stearylamine spectrum. Due to the fact that NH stretching and bending vibrations of primary, secondary, and tertiary amine had tiny differences, it usually showed two peaks for primary amine, one peak for secondary amine, and no peak for tertiary amine. Moreover, the NH bending band of primary amine will be intense, thus, seldom seen in secondary amine. As a result, exhibition of the single broad peak with lower intensity around 3,500–3,200 cm^{-1} and the diminishing of NH bending peak between 1,650 and 1,580 cm^{-1} could be used to draw the conclusion that stearylamine and mannose had covalently conjugated by secondary amine bond.

It is shown in Fig. 2 that the chemical shift of mannose proton at different positions of C_1 to C_6 varied from δ 4.60 to 3.90 ppm and no chemical shift was found at lower than δ 3.9 ppm. Nevertheless, the chemical shift of synthesized SAMAN dramatically showed the long alkyl chain proton at δ 1.28 ppm and small intensity of –NH– proton at δ 2.12 ppm. This small intensity was due to the presence of secondary amine linkage at the anomeric carbon atom of mannose molecules which could be used to confirm the glycosylation of mannose with long-chain octadecyl amine. Besides, the multiplex at chemical shift of δ 3.83 ppm and duplet at δ 4.45 ppm would indicate the β and α form of SAMAN, respectively, as described earlier (11).

The percentage residual amount of mannose was found to be 0.96±0.23% whereas that of stearylamine was 0.41±0.04% by weight of SAMAN.

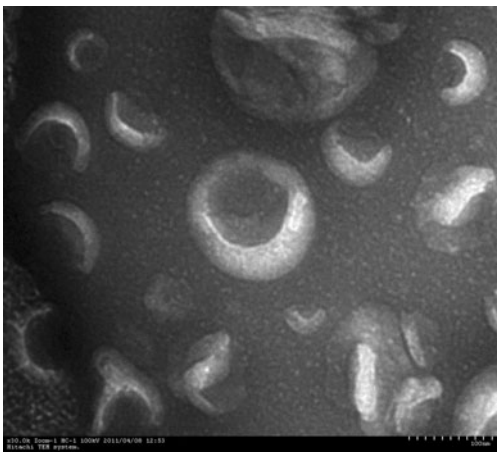

Fig. 3. Transmission electron photomicrograph of mannosylated-0.75 LZ liposomes. Magnification: ×30,000

Table I. Particle size, Polydispersity Index (PDI), Zeta Potential, %EE, %LC, %Cumulative Amount Permeated After 3 h, and Apparent Permeability Coefficient (P_{app}) of Various Formulations of Mannosylated LZ Liposomes with PC/Chol Molar Ratio of 8:2

Formulation	Mean (SD) [a]						
	Particle size (nm)	PDI	Zeta potential (mV)	%EE	%LC	%Cumulative amount permeated after 3 h	P_{app} ($\times 10^6$ cm/s)
LZ solution	–		–	–	–	0.28 (0.07)	0.14 (0.03)
LZ liposomes	390.3 (65.1)	0.375 (0.060)	−23.28 (3.90)[b]	27.86 (1.55)	4.44 (0.25)	1.53 (0.63)	0.39 (0.16)
Mannosylated-0.5 LZ liposomes	234.7 (3.2)	0.323 (0.040)	−25.80 (5.52)	14.10 (0.24)	2.77 (0.05)	2.12 (1.25)	0.17 (0.04)
Mannosylated-0.75 LZ liposomes	290.8 (0.2)	0.435 (0.013)	−19.08 (2.30)	10.09 (0.27)	1.90 (0.05)	3.20 (0.23)	0.97 (1.44)[c]
Mannosylated-1 LZ liposomes	431.0 (88.2)	0.452 (0.020)	−10.97 (1.71)	7.52 (0.92)	1.44 (0.17)	2.05 (0.81)	0.54 (0.59)

[a] Average from three determinations
[b] Significantly different from blank negatively charged liposomes [−33.43 (1.25)] ($p<0.05$, independent student pair t test)
[c] Significantly different from LZ solution, LZ liposomes, and mannosylated-0.5 LZ liposomes ($p<0.05$, Dunnett T3)

Physicochemical Characterization of Manosylated LZ Liposomes

The TEM image of mannosylated-0.75 LZ liposomes is shown in Fig. 3. The existence of the phospholipid bilayer could be visualized by the lamellar structure which appeared to be the type of oligolamellar vesicles.

Particle sizes of mannosylated LZ liposomes prepared in this study were in the range of 234.7–431.0 nm as shown in Table I. It was obviously shown that incorporation of more SAMAN into LZ liposomes generally yielded larger particles. The long chain of SAMAN could exhibit the insertion capability into lipid bilayer and exposed the hydrophilic polar head of mannose to the surface. Mannose domains on the surface might act as a hindrance for compacting arrangement between DCP and PC, which would be pronounced at higher SAMAN molar ratio. Moreover, the inclusion of SAMAN into lipid bilayer could compete with DCP molecules during the lipid film hydration, resulting in reduced DCP in lipid vesicles as SAMAN molar ratio was increased. On the other hand, LZ liposomes were shown to have comparable size with mannosylated-1 LZ liposomes. This might be due to the fact that lysozyme was entrapped predominantly by interact with lipid bilayer via ionic interaction on the surface of liposomes.

The zeta potentials of LZ liposomes in Table I demonstrated that LZ imposed strong influence on the net surface charge of negatively charged liposomes. Since LZ is a highly basic protein with isoelectric point (pI)=11.16 (16), it would exhibit positive charge at pH 7.4 used and certainly exert electrostatic Coulombic interaction with the negatively charged bilayer membrane as previously suggested (17).

In addition, SAMAN containing liposomes expressed the more reduction of negative charge with increasing SAMAN molar ratios. SAMAN is a long-chain glycosylamine with octadecyl hydrocarbon, and also has a positive charge of $-NH_3^+$ group. This long alkyl chain could be inserted and competed with DCP, leading to reduction of the amount of DCP in lipid bilayer. The consequence of both outcomes of competitive insertion and the positive charge of $-NH_3^+$ group would result in dramatic decline in negative zeta potential of SAMAN containing liposomes.

It can clearly be seen from Table I that all formulations of mannosylated LZ liposomes exhibited lower %EE than that of

Fig. 4. The percent cumulative amount transported across Caco-2 cell monolayers of LZ solution (*diamond*), LZ liposomes (*square*), and mannosylated-0.75 LZ liposomes (*asterisk*)

LZ liposomes, which could be explained by electrostatic interaction as discussed earlier. It has recently been reported that positive charge LZ was far more entrapped in negatively charged liposomes than in non-charged ones. The ionic interaction was pronounced at the liposomal surface which was evident by alteration of ^{31}P NMR chemical shift of PC in lipid bilayer (17). Moreover, %EE of SAMAN-containing liposomes was gradually declined with increasing SAMAN molar ratio from 14.10 to 10.09% and to 7.52% for mannosylated-0.5, mannosylated-0.75, and mannosylated-1 LZ liposomes, respectively. The insertion capability of SAMAN into lipid bilayer due to long alkyl chain was able to diminish the possibility of DCP to be incorporated into lipid vesicles during the hydration process, and hence, less negative surface charge and entrapment.

Permeation Across Caco-2 Cell Monolayers

The permeation profiles across Caco-2 cell monolayers (Fig. 4) revealed that LZ solution could hardly permeate at only 0.28% after 3 h with the apparent permeability coefficient (P_{app}) of 0.14×10^{-6} cm/s (Table I). The permeability of LZ could significantly be increased about 2.8-folds by incorporating in liposomes ($p<0.05$, Dunnett T3). Such results suggested that conventional liposomes could possibly enhance GI absorption of protein drugs *via* the proposed interaction mechanism with enterocytes as previously reported, including stable adsorption, endocytosis, fusion, and lipid transfer (3,4,7,18).

In the case of mannosylated LZ liposomes, significant increases in permeability across Caco-2 cells monolayer compared to that of LZ solution were also observed in all formulations. With varying SAMAN molar ratio, the maximum permeability was found for mannosylated-0.75 LZ liposomes (Fig. 4), whose P_{app} were significantly (11- and 2-fold) higher than those of LZ solution and LZ liposomes ($p<0.05$, Dunnett 3). Moreover, P_{app} of mannosylated-1 LZ liposomes and mannosylated-0.5 LZ liposomes were enhanced to be 3.9- and 1.2-fold higher than that of LZ solution, respectively. The improved permeability of mannosylated LZ liposomes might be attributed to the interaction of terminal mannose unit with some kind of specific binding on the epithelial cells as previously suggested (19).

The differences in permeability among mannosylated LZ liposomes in this study could be explained on the basis of the effect of mannose density on the surface of mannosylated o/w emulsion previously studied (8). At 0.50 molar ratio of SAMAN, liposomes might have less mannosylated surface than that of 0.75 molar ratio, resulting in lower permeation in spite of higher entrapment efficiency. On the other hand, the lower entrapment efficiency and larger size of 430 nm in the case of 1.0 molar ratio of SAMAN might be the obstacle to LZ permeation *via* Caco-2 cells despite the elevated mannosylated surface. This may be attributed to the size-dependent adsorptive endocytosis of the intestinal enterocytes, in which 0.1-μm size had a significantly higher efficiency of uptake by intestinal tissues of both Peyer's patch and non-patch area than that of larger size particles (18). According to their results, 0.1-μm size exhibited higher uptake with increasing concentration and temperature, which implied that the uptake was active process, probably endocytosis. It was suggested that the smaller liposomes required less energy for movement which brought about more collision frequency and high permeability coefficient than larger liposomes did (20).

CONCLUSION

N-octadecyl-D-mannopyranosylamine(SAMAN) was synthesized in-house and characterized by FTIR and NMR. Mannosylated LZ liposomes were prepared by the use of SAMAN, the mean sizes, zeta potentials, drug entrapment efficiencies, and loading capacities of which were around 200–400 nm, −20 mV, 7–14%, and 2–4%, respectively. The permeations across Caco-2 cell monolayers of mannosylated LZ liposomal formulations were demonstrated to be substantially enhanced compared to conventional LZ liposomes and solution.

ACKNOWLEDGMENTS

Financial support from the Thailand Research Fund (TRF) through the Royal Golden Jubilee Ph.D. Program (grant no. PHD/0111/2546) is gratefully acknowledged. The authors wish to thank Faculty of Pharmacy and Faculty of Graduate Studies, Mahidol University, for research assistant scholarship (academic year 2009).

REFERENCES

1. Gabor F, Bogner E, Weissenboeck A, Wirth M. The lectin-cell interaction and its implications to intestinal lectin-mediated drug delivery. Adv Drug Del Rev. 2004;56:459–80.
2. Sarmento B, Ferreira DC, Jorgensen L, Van De Weert M. Probing insulin's secondary structure after entrapment into alginate/chitosan nanoparticles. Eur J Pharm Biopharm. 2007;65:10–7.
3. Song K-H, Chung S-J, Shim C-K. Preparation and evaluation of proliposome containig salmon calcitonin. J Controlled Release. 2002;84:27–37.
4. Song K-H, Chung S-J, Shim C-K. Enhanced intestinal absorption of salmon calcitonin (sCT) from proliposomes containing bile salts. J Controledl Release. 2005;106:298–308.
5. Yamabe K, Kato Y, Onishi H, Machida Y. Potentiality of double liposomes containing salmon calcitonin as oral dosage form. J Controlled Release. 2003;89:429–36.
6. Russell-Jones GJ, Veitch H, Arthur L. Lectin-mediated transport of nanoparticles across Caco-2 and OK cells. Int J Pharm. 1999;190:165–74.
7. Florence AT. The oral absorption of micro- and nanoparticles: neither exceptional nor unusual. Pharm Res. 1997; 14:259–66.
8. Yeeprae W, Kawakami S, Yamashita F, Hashida M. Effect of mannose density on mannose-receptor-mediated cellular uptake of mannosylated O/W emulsions by macrophages. J Controlled Release. 2006;114:193–201.
9. Wagner S, Lynch NJ, Walter W, Schwaeble WJ, Loos M. Differential expression of the murine mannose-binding lectins A and C in lymphoid and nonlymphoid organs and tissues. J Immunol. 2003;170:1462–5.
10. Uemura K, Saka M, Nakagawa T, Kawasaki N, Thiel S, Jensenius JC, *et al*. L-MBP is expressed in epithelial cells of mouse small intestine. J Immunol. 2002;169:6945–50.
11. Lockhoff O, Stadler P. Syntheses of glycosylamides as glycolipid analogs. Carbohydr Res. 1998;314:13–24.
12. Rakotomanga S, Baillet A, Pellerin F, Baylocq-Ferrier D. Liquid chromatographic analysis of monosaccharides with phenylisocyanate derivatization. J Pharm Biomed Anal. 1992;10:587–91.
13. Björkqvist B. Separation and determination of aliphatic and aromatic amines by high-performance liquid chromatography with ultraviolet detection. J Chromatogr. 1981;204:109–14.

14. Peterson GL. A simplification of the protein assay method of Lowry *et al.* which is more generally applicable. Anal Biochem. 1977;83:346–56.
15. Liao YH, Brown MB, Martin GP. Turbidimetric and HPLC assays for the determination of formulated lysozyme activity. J Pharm Pharmacol. 2001;53:549–54.
16. Kuehner DE, Engmann J, Fergg F, Wernick M, Blanch HW, Praus-nitz JM. Lysozyme net charge and ion binding in concentrated aqueous electrolyte solutions. J Phys Chem. 1999;B103:1368–74.
17. Witoonsaridsilp W, Panyarachun B, Sarisuta N, Müller-Goymann CC. Influence of microenvironment and liposomal formulation on secondary structure and bilayer interaction of lysozyme. Colloids Surf B Biointerfaces. 2010;75:501–9.
18. Takeuchi H, Matsui Y, Sugihara H, Yamamoto H, Kawashima Y. Effectiveness of submicron-sized, chitosan-coated liposomes in oral administration of peptide drugs. Int J Pharm. 2005;303:160–70.
19. Russell-Jones GJ. The potential use of receptor-mediated endocytosis for oral drug delivery. Adv Drug Del Rev. 1996;20:83–97.
20. Boonyapiwat B, Sarisuta N, Kunastitchai S. Characterization and *in vitro* evaluation of intestinal absorption of liposomes encapsulating zanamivir. Curr Drug Del. 2011;8:392–7.